



Published in final edited form as:

ACS Macro Lett. 2018 October 16; 7(10): 1174–1179. doi:10.1021/acsmacrolett.8b00625.

Quantitative and Mechanistic Mechanochemistry in Ferrocene Dissociation

Ye Sha^{#†}, Yudi Zhang^{#‡}, Enhua Xu[§], Zi Wang[‡], Tianyu Zhu[†], Stephen L. Craig^{*‡}, and Chuanbing Tang^{*†}

[†]Department of Chemistry and Biochemistry, University of South Carolina, Columbia, South Carolina 29208, United States

[‡]Department of Chemistry, Duke University, Durham, North Carolina 27708, United States

[§]Graduate School of System Informatics, Kobe University, Kobe 657-8501, Japan

[#] These authors contributed equally to this work.

Abstract

Ferrocene is classically regarded as being highly inert owing to the large dissociation energy of metal-cyclopentadienyl (Cp) bonds. We show that the Fe-Cp bond in ferrocene is the preferential site of mechanochemical scission in the pulsed ultrasonication of main-chain ferrocene-containing polybutadiene-derived polymers. Quantitative studies reveal that the Fe-Cp bond is similar in strength to the carbon-nitrogen bond of an azobisdialkyl nitrile (bond dissociation energy < -0 kcal/mol), despite the significantly higher Fe-Cp bond dissociation energy (approximately 90 kcal/mol). Mechanistic studies are consistent with a predominately heterolytic mechanism of chain scission. DFT calculations provide insights into the origins of ferrocene's mechanical lability.

Graphical Abstract

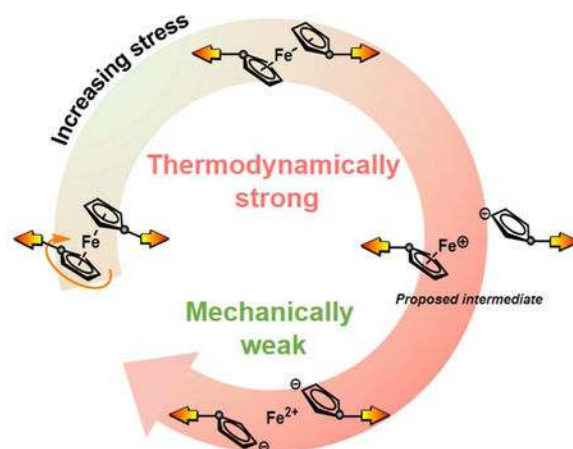
*Corresponding Author tang4@mailbox.sc.edu (C. Tang), stephen.craig@duke.edu (S.L.Craig).

Publisher's Disclaimer: This document is confidential and is proprietary to the American Chemical Society and its authors. Do not copy or disclose without written permission. If you have received this item in error, notify the sender and delete all copies.

ASSOCIATED CONTENT

Supporting Information

The Supporting Information is available free of charge on the ACS Publications website. Experimental details, synthetic procedures, computational details and characterization data.



Since ferrocene was discovered in the early 1950s, its captivating structure, reactivity and properties have led it to become one of the most classical organometallic compounds to date.^{1–4} Ferrocene's broad utility is due in large part to the stability of the iron-cyclopentadienyl (Fe-Cp) bond, the bond dissociation energy (BDE) of which (reported up to be 91 kcal/mol) approaches that of conventional covalent C-C bonds.⁵ As such, the ferrocene core is often assumed to be inert, enabling its utility in a wide range of material, electrochemical, and catalytic applications.^{4, 6–13}

Inspired by recent work in covalent polymer mechanochemistry,^{14–22} we wondered whether the Fe-Cp coordination bond could be broken efficiently and selectively through the application of mechanical force. And if so, what is the mechanism of the mechanochemical dissociation, and how does the mechanical strength of the organometallic Fe-Cp bond compare to that of organic covalent bonds of similar BDE? Not surprisingly, the allure of ferrocene as a potential mechanophore has captured the attention of others as well. Giannantonio et al. recently reported that main-chain ferrocene acts as a preferred site of mechanochemical chain scission in polyurethane and polyacrylate polymers, leading to the release and oxidation of iron to Fe³⁺.²³ Here, we report our own studies of ferrocene mechanochemistry and demonstrate that ferrocene is an efficient mechanophore in polybutadiene-derived polymers as well. We reasoned that the further development of this promising new class of mechanophores will benefit from quantitative mechanistic insights, and so we additionally set out to answer to several open questions: (1) Whether ferrocene dissociation might lead to the release and capture Fe²⁺ rather than Fe³⁺ as observed by Giannantonio et al.? (2) What is the fate of the dissociation Cp ligand? (3) How does the mechanical strength of the Fe-Cp bond compare to that of other mechanically labile bonds? (4) More generally, what is the mechanism of the mechanochemical dissociation? Is it heterolytic or homolytic? A combination of experimental and computational techniques is used to probe these questions, and the results suggest strategies for expanding the utility of this promising class of multifunctional metallomechanophores.

Multi-mechanophore polymers are known to facilitate the characterization and quantification of mechanophore reactivity, in ways that provide advantages over a single mechanophore labeling strategy,^{23–25} and we followed a well-established methodology of using entropy

driven ring-opening metathesis polymerization (ED-ROMP) to synthesize polymers of varying molecular weight and mechanophore content (Table 1; see SI for synthetic details).^{26, 27}

We first investigated the sono-mechanochemistry of **P1** ($M_n = 111,500$ Da; 1 mg/mL in THF), a copolymer of 5-methoxycyclooctene and a ferrocene macrocycle **4** (Figure 1b). The molecular weight decreases with sonication time (Figure 1c) until reaching an apparent limiting molecular weight of $M_{lim} = 17,600$ Da (Figure S1). The formation of dissociated Cp ligand is revealed by ^1H NMR spectroscopy ($\delta = 6.4\text{--}7.5$ ppm, Figure 1d),^{28, 29} and the peak intensity increases with sonication time. We hypothesize that the Cp originated from protonation of mechanically generated cyclopentadienyl anions.³⁰ Support for this hypothesis is found through the addition of isopropyl alcohol (10 vol%) to the sonication solution, which significantly increased the yield of the free ligand (Figure S2). Thus, this observation suggested that the mechanism of ferrocene dissociation involves the heterolytic dissociation of Cp^- from $[\text{CpFe}]^+$ and inspired further mechanistic studies (vide infra).

As observed by Giannantonio et al., the chain scission is quite specific to the embedded ferrocene units.²³ A comparison of the number of chain scission events (quantified by gel permeation chromatography) and the number of ferrocene scission events (quantified by ^1H NMR) revealed that $97 \pm 3\%$ of the scission events occur at ferrocene (see Figures S3).

This selectivity hints at unexpectedly high lability of the Fe-Cp bond, and we quantified the mechanical bond strength of ferrocene by adding *gem*-dichlorocyclopropane (*gDCC*) mechanophores into the same polymer backbone (**P4**, Table 1). As some of us have reported previously,^{31, 32} the *gDCC* mechanophores serve as an internal standard for estimating the scission bond strength, through the competing mechanochemical processes of *gDCC* ring opening and ferrocene scission as shown in Figure 2a. The fraction of *gDCC*s that ring open per number of scission cycles of the parent polymer, Φ_i , has been shown to be a robust indicator of the mechanical strength of the bonds that break (here, the Fe-Cp bond) during polymer sonication.³³ As seen in Figure 2b, Φ_i of **P4** ($\Phi_i = 0.22$) is considerably lower than that of dichlorocyclopropanated polybutadiene **P3**, which lacks the ferrocene ($\Phi_i = 0.79$); ferrocene is demonstrably more mechanically labile than the carbon-carbon bonds of polybutadiene. Similarly, control polymer **P5** ($\Phi_i = 0.62$) confirms that the ferrocene mechanophore is also more labile than the bonds associated with the aryl ester linkages

Because they are robust over a range of experimental sonication conditions, the Φ_i values allow us to compare the mechanical strength (in ultrasound) of ferrocene to that of other scissile, covalent bonds. Lee et al. recently reported the mechanical strength of the carbon-nitrogen bond of an azobisdialkyl nitrile (BDE < 30 kcal/mol; $\Phi_i = 0.18$), the carbon-sulfur bond of a thioether (BDE = 71–74 kcal/mol; $\Phi_i = 0.43$), and the carbon-oxygen bond of a benzylphenyl ether (BDE = 52–54 kcal/mol; $\Phi_i = 0.62$).³¹ Interestingly, ferrocene has a mechanical strength that is very similar to that of an azobisdialkyl nitrile, despite the fact that its reported thermodynamic bond strength is nearly three times as large and even greater than that of a thioether or benzylphenyl ether. We note that the trend in Φ_i values are verified by a similar trend in M_{lim} (see Table S2).

We next consider further the chain scission mechanism of ferrocene, and in particular whether Cp dissociation involves back electron transfer from the Cp anion to Fe. Giannantonio et al. trapped released Fe^{3+} ions using KSCN, suggestive of the same heterolytic dissociation mechanism implied by our above observation of protonated Cp.²³ This mechanism is also consistent with the accepted mechanism for formation of ferrocene, although under different conditions. The generation of Fe^{3+} , however, requires an unspecified oxidative process, which leaves some ambiguity as to the oxidation state of the iron formed directly from the mechanical dissociation. We therefore probed further the contributions from two possible mechanisms: heterolytic or homolytic,³⁴ as shown in Figure 3a.

If the mechanism was heterolytic, as suggested by the observations noted above, then the dissociation energy would include a contribution from the charge separation of $[\text{CpFe}]^+$ and Cp^- in the relative low dielectric THF solvent. We therefore added soluble tetrabutylammonium bromide (TBAB) salt to the mixture in order to stabilize any charge separation and/or assist in anionic ligand exchange. As shown in Figure 3b, the addition of TBAB lowers Φ_i further to 0.12 (the ferrocene is now measurably weaker than the azobisdialkyl nitrile), consistent with a heterolytic mechanism. Importantly, a control experiment demonstrates that the influence of TBAB is specific to the ferrocene, Φ_i does not change for poly *g*DCC (Figure 3c).

We also consider the fate of the iron. Phenanthroline associates with ferrous ion to form a stable complex $[\text{Fe}(\text{phenanthroline})_3]^{2+}$ that produces a strong absorption in DMF solutions that,³⁵ at ~510 nm, is well separated from the characteristic absorption of ferrocene derivatives (~450 nm). We therefore synthesized a DMF-soluble copolymer of ferrocene and 5-hydroxycyclooctene (**P7**). **P7** is almost identical in strength with **P4** in THF (see Figure S4). Sonication of **P7** alone produces no change in solution color or UV-Vis spectrum. Sonication of **P7** in the presence of phenanthroline, however, leads to a peak at 510 nm (Figure 3d) that matches that of independently prepared $[\text{Fe}(\text{phenanthroline})_3]^{2+}$. A control experiment was carried out under the same conditions by mixing homopolymer **P8** and ferrocene small molecules (Compound **6**, see SI) at the same concentration of ferrocenyl units as **P7** in DMF. Sonication produces no change in the absorption spectrum and provides strong evidence that the peak located at 510 nm in Figure 3d is due to the capture of mechanically generated ferrous ions. Interestingly, an additional peak ($\lambda_{\text{max}} = 620 \text{ nm}$) also appears in response to sonication of **P7**, giving the solution a purple tint (Figure 3d). This peak might be attributed to a complex formed by half-sandwich ferrocenium and phenanthroline after chain scission, which is very similar to a reported half-sandwich ferrocenium acetonitrile intermediate with purple color and absorption band red shift by 100 nm relative to that of ferrocene.^{36, 37} This intermediate is unstable and decomposes to release ferrous ion gradually as shown in Figure S5, complicating further characterization. Nonetheless, these observations are consistent with initial heterolytic dissociation to $[\text{CpFe}]^+$ and Cp^- .

We also looked for evidence of homolytic dissociation, reasoning that we should be able to trap cyclopentadienyl radicals through radical addition reactions using methods some of us have employed successfully before.^{38, 39} **P1** was carbon-centered radicals.⁴⁰ The rate of

sonochemical molecular weight degradation did not change with addition of TEMPO, nor were any new peaks observed in the ^1H NMR spectra that would support the incorporation of TEMPO moiety in the polymer chain ends (see Figures S6 and S7). Taken together, we conclude that mechanical dissociation of ferrocene proceeds through a predominately heterolytic dissociation pathway, which is scarcely reported in mechanically-induced bond cleavage.^{15, 24, 41–43}

To further probe the stretching and breaking process at an atomistic level, DFT calculations were performed with a constrained geometry simulates external force (COGEF) method.^{44–46} As shown in Figure 4a, two Cp groups are aligned in an eclipsed geometry in the most energetically favorable state in the absence of applied force. As the ferrocene is stretched, the cyclopentadienyl rings start to twist until a fully staggered geometry is reached. Subsequent stretching distorts bond angles and bond lengths, and the energy of the system increases until Cp dissociates. Clearly, the dissociation process also supports the generation of Cp^- and $[\text{CpFe}]^+$ as experimentally observed.

These calculations likely overestimate the dissociation energies, but nonetheless provide some key insights. Most sonicated in the presence of TEMPO (32 mM), which efficiently traps notably, the Fe-Cp is quite “soft,” and so the energy increases over a fairly long dissociation coordinate. One consequence of this is that the maximum force on the calculated potential energy surface (corresponding the force necessary to reach a barrier-less process) is only 3.1 nN, which suggests an upper limit for the ferrocene dissociation force that is much lower than that of conventional covalent bonds in organic compounds.⁴⁴ Similarly, as Cp dissociation occurs, the force is applied over a large distance and therefore contributes more energy through work to the reaction, effectively lowering the force-coupled activation energy to a greater extent. The calculations are consistent with the low force for dissociation on the microsecond timescale as revealed by our experimental observations.^{31, 44, 47} Applying models employed previously by Lee et al.,³¹ the characteristic breaking force for ferrocene is likely comparable to the relevant ring opening force of the *g*DCC mechanophore (~2 nN), although it is not clear how accurate these models are at low forces such as those observed here. Regardless, the forces required for ferrocene dissociation are very likely low enough that they can be probed using more precise techniques such as single molecule force spectroscopy (SMFS). Vancso and co-workers utilized SMFS experiments on ferrocene-containing polymers as a redox-driven single macromolecular motor.⁴⁸ However, they did not observe the dissociation of ferrocene due to insufficient mechanical stress. Further refinement on SMFS for main-chain ferrocene-containing polymers might be worthy for exploration. that are inert over long time in the absence of large mechanical forces but might be quite sensitive to high loads. Because the dissociation produces highly reactive and redox active products with differential properties, ferrocene might be a useful mechanophore for a range of material applications, including biomedical uses that capitalize on the rich biochemistry of iron. The mechanical susceptibility, mechanism, and products of mechanically triggered ferrocene scission are likely to depend very much on the specific use environment, and the quantitative and mechanistic studies reported here should provide baseline information and strategies for similar investigations on related systems. Finally, we speculate that striking mechanical sensitivity of the Fe-Cp bond might be general for the

metallocene architecture, leading to opportunities to broaden this approach to a wide range of metals.

Supplementary Material

Refer to Web version on PubMed Central for supplementary material.

ACKNOWLEDGMENT

This work is partially supported by the National Institutes of Health (R01AI120987 to C.T.) and by the US Army Research Laboratory and the Army Research Office (Grant W911NF-15-0143 to S.L.C).

These results demonstrate that ferrocene possesses a mechanical susceptibility that belies its thermodynamic stability, creating opportunities for use in polymeric materials

REFERENCES

- (1). Wilkinson G; Rosenblum M; Whiting MC; Woodward RB The structure of iron bis-cyclopentadienyl. *J. Am. Chem. Soc* 1952, 74, 2125–2126.
- (2). Fischer EO; Pfab W Cyclopentadiene-metallic complex, a new type of organo-metallic compound. *Naturforsch B* 1952, 7, 377–379.
- (3). Foucher DA; Tang BZ; Manners I Ring-opening polymerization of strained, ring-tilted ferrocenophanes: a route to high-molecular-weight poly (ferrocenylsilanes). *J. Am. Chem. Soc* 1992, 114, 6246–6248.
- (4). Astruc D Why is Ferrocene so Exceptional? *Eur. J. Inorg. Chem* 2017, 6–29.
- (5). Lewis KE; Smith GP Bond dissociation energies in ferrocene. *J. Am. Chem. Soc* 1984, 106, 4650–4651.
- (6). Yan Y; Zhang JY; Ren LX; Tang CB Metal-containing and related polymers for biomedical applications. *Chem. Soc. Rev* 2016, 45, 5232–5263. [PubMed: 26910408]
- (7). Hailes RLN; Oliver AM; Gwyther J; Whittell GR; Manners I Polyferrocenylsilanes: synthesis, properties, and applications. *Chem. Soc. Rev* 2016, 45, 5358–5407. [PubMed: 27348354]
- (8). Hardy CG; Zhang JY; Yan Y; Ren LX; Tang CB Metallopolymers with transition metals in the side-chain by living and controlled polymerization techniques. *Prog. Polym. Sci* 2014, 39, 1742–1796.
- (9). Fu GC Enantioselective nucleophilic catalysis with “planar-chiral” heterocycles. *Accounts. Chem. Res* 2000, 33, 412–420.
- (10). Nguyen P Gomez-Elipe P Manners I Organometallic polymers with transition metals in the main chain. *Chem. Rev* 1999, 99, 1515–1548. [PubMed: 11849001]
- (11). Hardy CG; Ren LX; Zhang JY; Tang CB Side-Chain Metallocene-Containing Polymers by Living and Controlled Polymerizations. *Israel J. Chem* 2012, 52, 230–245.
- (12). Pietschnig R Polymers with pendant ferrocenes. *Chem. Soc. Rev* 2016, 45, 5216–5231. [PubMed: 27156979]
- (13). Gallei M; Ruttiger C Recent Trends in Metallopolymer Design: Redox-Controlled Surfaces, Porous Membranes, and Switchable Optical Materials Using Ferrocene-Containing Polymers. *Chem.-Eur. J* 2018, 24, 10006–10021.
- (14). Simon YC; Craig SL, *Mechanochemistry in Materials*. Royal Society of Chemistry: 2017; Vol. 26.
- (15). Caruso MM; Davis DA; Shen Q; Odom SA; Sottos NR; White SR; Moore JS Mechanically-Induced Chemical Changes in Polymeric Materials. *Chem. Rev* 2009, 109, 5755–5798. [PubMed: 19827748]
- (16). Black AL; Lenhardt JM; Craig SL From molecular mechanochemistry to stress-responsive materials. *J. Mater. Chem* 2011, 21, 1655–1663.

- (17). Balkenende DWR; Coulibaly S; Balog S; Simon YC; Fiore GL; Weder C Mechanochemistry with Metallosupramolecular Polymers. *J. Am. Chem. Soc* 2014, 136, 10493–10498. [PubMed: 24972163]
- (18). James SL; Adams CJ; Bolm C; Braga D; Collier P; Friscic T; Grepioni F; Harris KDM; Hyett G; Jones W; Krebs A; Mack J; Maini L; Orpen AG; Parkin IP; Shearouse WC; Steed JW; Waddell DC Mechanochemistry: opportunities for new and cleaner synthesis. *Chem. Soc. Rev* 2012, 41, 413–447. [PubMed: 21892512]
- (19). Larsen MB; Boydston AJ “Flex-Activated” Mechanophores: Using Polymer Mechanochemistry To Direct Bond Bending Activation. *J. Am. Chem. Soc* 2013, 135, 8189–8192. [PubMed: 23687904]
- (20). Chen Z; Mercer JAM; Zhu X; Romaniuk JAH; Pfattner R; Cegelski L; Martinez TJ; Burns NZ; Xia Y Mechanochemical unzipping of insulating poly(ladderene) to semiconducting polyacetylene. *Science* 2017, 357, 475–478. [PubMed: 28774923]
- (21). De Bo G Mechanochemistry of the mechanical bond. *Chemical Science* 2018, 9, 15–21. [PubMed: 29629069]
- (22). Akbulatov S; Tian Y; Huang Z; Kucharski TJ; Yang QZ; Boulatov R Experimentally realized mechanochemistry distinct from force-accelerated scission of loaded bonds. *Science* 2017, 357.
- (23). Di Giannantonio M; Ayer MA; Verde-Sesto E; Lattuada M; Weder C; Fromm KM Triggered metal ion release and oxidation: Ferrocene as new mechanophore in polymers. *Angew. Chem. Int. Ed* 2018, 130, 11616–11621.
- (24). Li J; Nagamani C; Moore JS Polymer Mechanochemistry: From Destructive to Productive. *Accounts. Chem. Res* 2015, 48, 2181–2190.
- (25). Bowser BH; Craig SL Empowering mechanochemistry with multi-mechanophore polymer architectures. *Polymer Chemistry* 2018, 3583–3593.
- (26). Grubbs RH; Chang S Recent advances in olefin metathesis and its application in organic synthesis. *Tetrahedron* 1998, 54, 4413–4450.
- (27). Pollino JM; Stubbs LP; Weck M Living ROMP of exo-norbornene esters possessing (PdSCS)-S-II pincer complexes or diaminopyridines. *Macromolecules* 2003, 36, 2230–2234.
- (28). Grunewald GL; Davis DP A new convenient synthesis of bridgehead substituted norbornenes. *J. Org. Chem* 1978, 43, 3074–3076.
- (29). Top S; Lehn JS; Morel P; Jaouen G Synthesis of cyclopentadienyltricarbonylrhenium(I) carboxylic acid from perrhenate. *J. Organomet. Chem* 1999, 583, 63–68.
- (30). Tanabe M; Vandermeulen GWM; Chan WY; Cyr PW; Vanderark L; Rider DA; Manners I Photocontrolled living polymerizations. *Nature Mater.* 2006, 5, 467–470. [PubMed: 16699511]
- (31). Lee B; Niu Z; Wang J; Slebodnick C; Craig SL Relative Mechanical Strengths of Weak Bonds in Sonochemical Polymer Mechanochemistry. *J. Am. Chem. Soc* 2015, 137, 10826–10832. [PubMed: 26247609]
- (32). Lenhardt JM; Black AL; Craig SL gem-Dichlorocyclopropanes as Abundant and Efficient Mechanophores in Polybutadiene Copolymers under Mechanical Stress. *J. Am. Chem. Soc* 2009, 131, 10818. [PubMed: 19603747]
- (33). Lenhardt JM; Ramirez ALB; Lee B; Kouznetsova TB; Craig SL Mechanistic Insights into the Sonochemical Activation of Multimechanophore Cyclopropanated Polybutadiene Polymers. *Macromolecules* 2015, 48, 6396–6403.
- (34). Pierloot K; Persson BJ; Roos BO Theoretical study of the chemical bonding in [Ni (C₂H₄)] and ferrocene. *J. Phys. Chem* 1995, 99, 3465–3472.
- (35). Fortune WB; Mellon MG Determination of iron with o-phenanthroline - A spectrophotometric study. *Ind. Eng. Chem. Anal. Ed* 1938, 10, 0060–0064.
- (36). Gill TP; Mann KR P Photochemistry of [(η -C₅H₅) Fe (η -p-xy)] PF₆ in acetonitrile solution. Characterization and reactivity of [(η -C₅H₅) Fe (MeCN) ₃]⁺. *Inorg. Chem* 1983, 22, 1986–1991.
- (37). Schrenk JL; McNair AM; McCormick FB; Mann KR Effect of arene methylation on photochemical arene replacement reactions of the iron and ruthenium complexes. *Inorg. Chem* 1986, 25, 3501–3504.

- (38). Klukovich HM; Kean ZS; Iacono ST; Craig SL Mechanically Induced Scission and Subsequent Thermal Remending of Perfluorocyclobutane Polymers. *J. Am. Chem. Soc* 2011, 133, 17882–17888. [PubMed: 21967190]
- (39). Lenhardt JM; Ong MT; Choe R; Evenhuis CR; Martinez TJ; Craig SL Trapping a Diradical Transition State by Mechanochemical Polymer Extension. *Science* 2010, 329, 1057–1060. [PubMed: 20798315]
- (40). Sobek J; Martschke R; Fischer H Entropy control of the cross-reaction between carbon-centered and nitroxide radicals. *J. Am. Chem. Soc* 2001, 123, 2849–2857. [PubMed: 11456972]
- (41). Aktah D; Frank I Breaking bonds by mechanical stress: When do electrons decide for the other side? *J. Am. Chem. Soc* 2002, 124, 3402–3406. [PubMed: 11916426]
- (42). Diesendruck CE; Peterson GI; Kulik HJ; Kaitz JA; Mar BD; May PA; White SR; Martinez TJ; Boydston AJ; Moore JS Mechanically triggered heterolytic unzipping of a low-ceiling-temperature polymer. *Nature Chem* 2014, 6, 624–629.
- (43). Shiraki T; Diesendruck CE; Moore JS The mechanochemical production of phenyl cations through heterolytic bond scission. *Faraday. Discuss* 2014, 170, 385–394. [PubMed: 25408164]
- (44). Beyer MK The mechanical strength of a covalent bond calculated by density functional theory. *J. Chem. Phys* 2000, 112, 7307–7312.
- (45). Groote R; Szyja BM; Pidko EA; Hensen EJM; Sijbesma RP Unfolding and Mechanochemical Scission of Supramolecular Polymers Containing a Metal-Ligand Coordination Bond. *Macromolecules* 2011, 44, 9187–9195.
- (46). Li Y; Haworth NL; Xiang L; Ciampi S; Coote ML; Tao N Mechanical Stretching-Induced Electron-Transfer Reactions and Conductance Switching in Single Molecules. *J. Am. Chem. Soc* 2017, 139, 14699–14706. [PubMed: 28946743]
- (47). Beyer MK; Clausen-Schaumann H Mechanochemistry: The mechanical activation of covalent bonds. *Chem. Rev* 2005, 105, 2921–2948. [PubMed: 16092823]
- (48). Zou S; Hempenius MA; Schonherr H; Vancso GJ Force spectroscopy of individual stimulus-responsive poly (ferrocenyldimethylsilane) chains: Towards a redox-driven macromolecular motor. *Macromol. Rapid Commun* 2006, 27, 103–108.

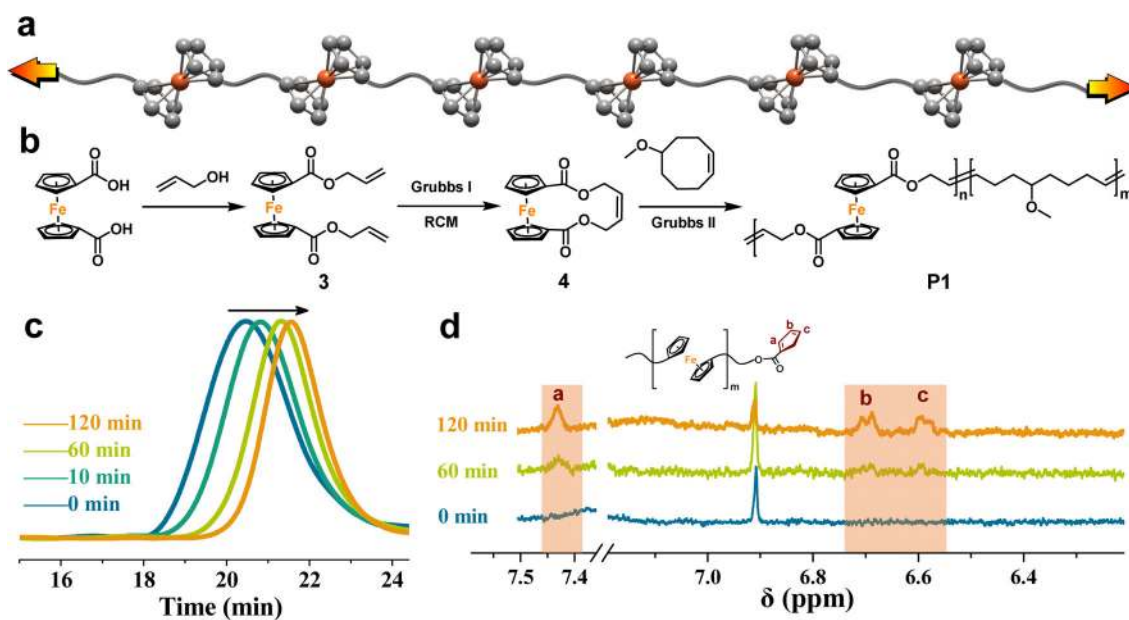


Figure 1.
 (a) Schematic illustration of a main-chain ferrocene-containing polymer exposed to external mechanical stress; (b) Representative synthetic scheme for main-chain ferrocene-containing polymer; (c) GPC traces of **P1** after sonication for different time. The arrow indicates the increase of sonication time; (d) Time-dependent ^1H NMR spectra of **P1** exposed to sonication.

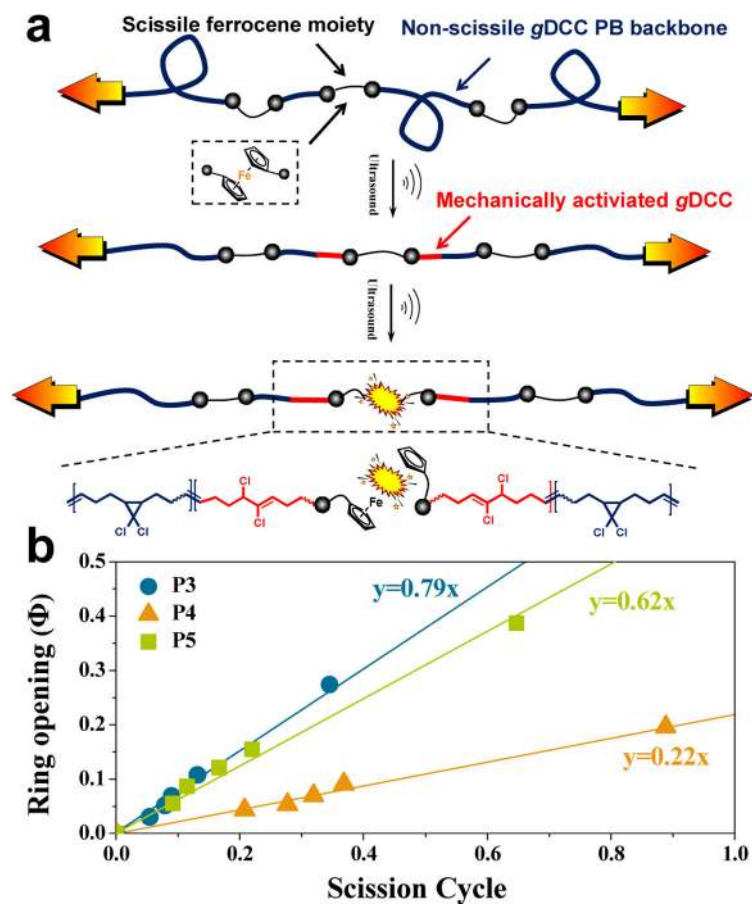


Figure 2.
 (a) Competing mechanochemical processes of gDCC ring opening and ferrocene scission;
 (b) Fraction of ring opening of gDCC versus scission cycle for **P3**, **P4** and **P5**.

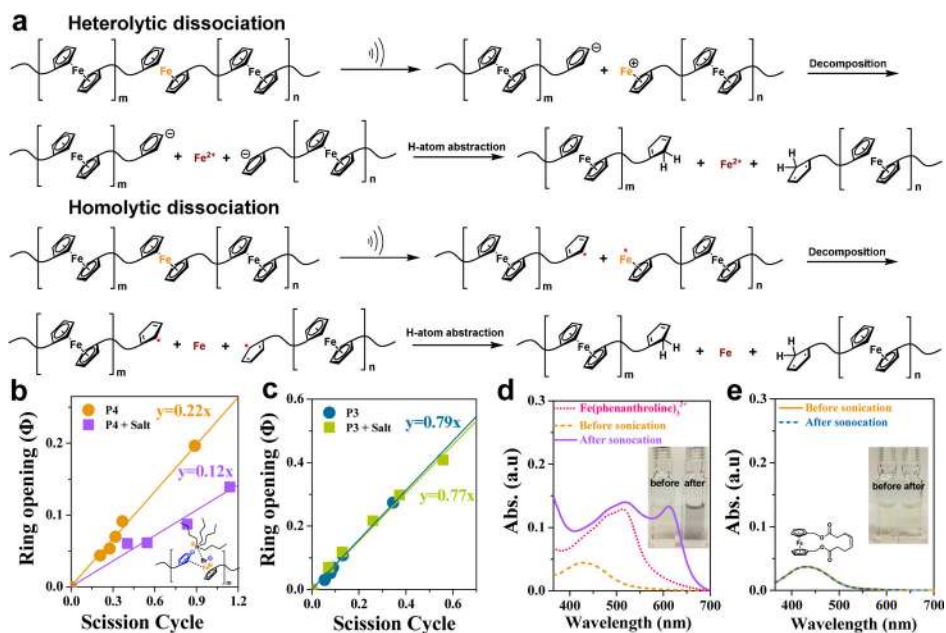


Figure 3. (a) Proposed heterolytic and homolytic dissociation mechanisms of a ferrocene-containing polymer by ultrasound-induced chain scission. (b) Ring-opening ratio of *g*DCC versus scission cycle for **P4** and organic salt-stabilized **P4**; (c) Ring-opening ratio of *g*DCC versus scission cycle for **P3** and organic salt-stabilized **P3**; (d) UV-vis absorption spectra of **P7** mixed with phenanthroline before and after sonication; (e) UV-vis absorption spectra of **P8** mixed with phenanthroline and cyclic ferrocenyl olefin monomer **6** before and after sonication.

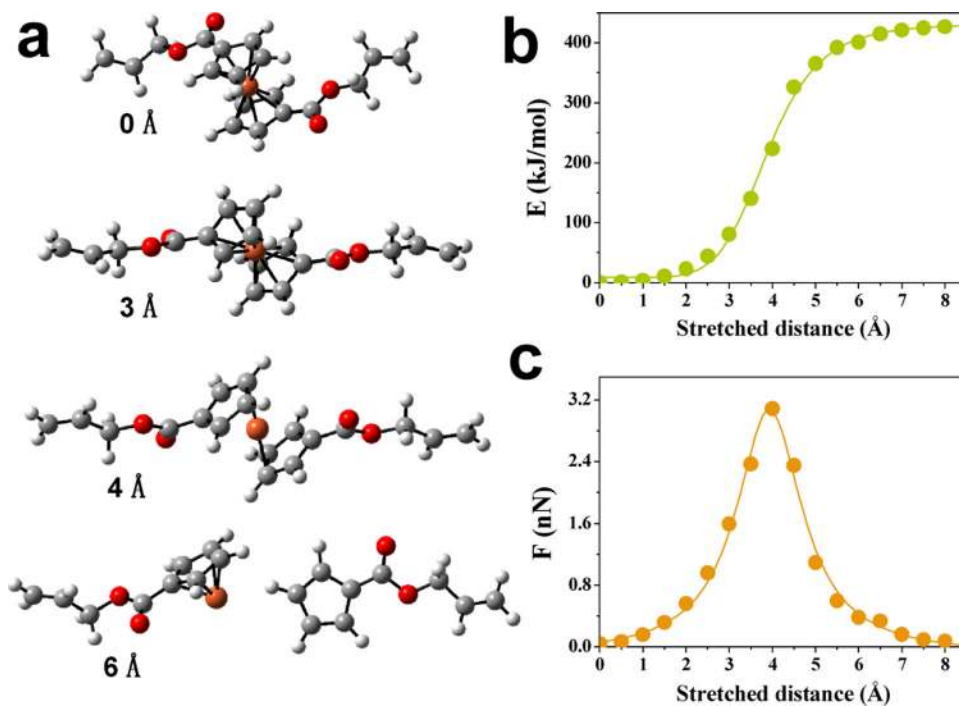
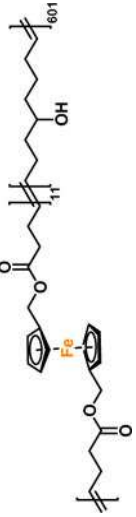
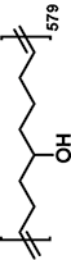


Figure 4. DFT predictions of a model compound of ferrocene during mechanical stretching: (a) Structural evolutions as the chain termini are stretched; (b) COGEF potential with the chain terminal distance varied from fully relaxed (0 Å) to 8 Å; (c) COGEF force with a fixed stretching distance.

Table 1

Polymers used in this study

Polymer	Architecture	M_n (Da)	D	Labeling molar ratio
P1		111,500	2.1	2%
P2		90,400	2.2	3%
P3		75,000	1.6	--
P4		97,000	1.6	10%
P5		92,000	1.7	9%
P6		75,000	1.5	8%

Polymer	Architecture	M_n (Da)	\bar{D}	Labeling molar ratio
P7		80,000	1.6	2%
P8		73,100	1.6	--